2024 IEEE/RSJ International Conference on Intelligent Robots and Systems (IROS)
October 14-18, 2024. Abu Dhabi, UAE

Construction of Musculoskeletal Simulation for Shoulder Complex with Ligaments and Its Validation via Model Predictive Control

Yuta Sahara[1], Akihiro Miki[1], Yoshimoto Ribayashi[1], Shunnosuke Yoshimura[1], Kento Kawaharazuka[1], Kei Okada[1], and Masayuki Inaba[1]

***Abstract*— The complex ways in which humans utilize their bodies in sports and martial arts are remarkable, and human motion analysis is one of the most effective tools for robot body design and control. On the other hand, motion analysis is not easy, and it is difficult to measure complex body motions in detail due to the influence of numerous muscles and soft tissues, mainly ligaments. In response, various musculoskeletal simulators have been developed and applied to motion analysis and robotics. However, none of them reproduce the ligaments but only the muscles, nor do they focus on the shoulder complex, including the clavicle and scapula, which is one of the most complex parts of the body. Therefore, in this study, a detailed simulation model of the shoulder complex including ligaments is constructed. The model will mimic not only the skeletal structure and muscle arrangement but also the ligament arrangement and maximum muscle strength. Through model predictive control based on the constructed simulation, we confirmed that the ligaments contribute to joint stabilization in the first movement and that the proper distribution of maximum muscle force contributes to the equalization of the load on each muscle, demonstrating the effectiveness of this simulation.**

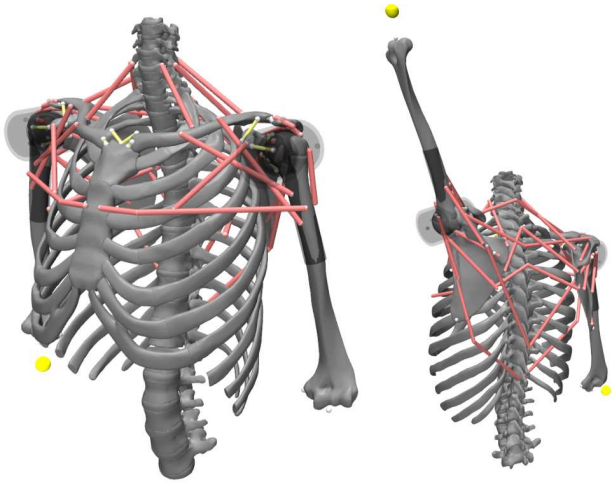

Fig. 1: Overview of the proposed musculoskeletal model.

I. Introduction

Humans make effective use of their bodies to achieve the complex movements seen in sports and martial arts. However, detailed analysis of how they move is difficult. This is because it is difficult to measure the contribution to movement of each of the more than 600 muscles in the human body. It is also difficult to measure the effects of soft tissues, mainly ligaments, which are greatly involved in joint movement. For these reasons, various musculoskeletal simulators have been developed and applied to motion analysis and robotics. However, existing musculoskeletal simulators have been constructed as simple models with a small number of muscles or without considering soft tissues such as ligaments. For example, in the model of Holzbaur et al. [1] the shoulder joint is configured as a joint that satisfies the regression equation obtained by de Groot et al. [2] by experimentally studying the shoulder bone interlocking, with 16 muscles belonging to the shoulder complex in one shoulder. In myoSuite's myoArm, the shoulder is configured as a multiple uniaxial rotational joint with 63 muscles in the entire single arm, of which 15 muscles belong to the shoulder complex in one shoulder [3]. There are also Kengoro [4], musculoskeletal humanoids, which are wire-driven robots that mimic human muscles. Kengoro does not have ligaments in the shoulder joints and must have tension on the surrounding muscles or it will dislocate. Furthermore, Musashi [5] is a humanoid that includes the advantages of wire drive in musculoskeletal humanoids such as Kengoro, but it does not have scapula on its shoulders and does not adopt the structure of the human shoulder.

In this study, a new musculoskeletal simulation model with soft tissue ligaments and the same number of muscles as a human was developed in order to apply the human shoulder structure, including its soft tissues and numerous muscles, to a musculoskeletal robot. In particular, the shoulder complex, which has the widest range of motion due to the function of muscles and ligaments, was the main target of the development. Ligaments were introduced to the joints in the same arrangement as in the human body, and 20 muscles were placed in one shoulder, for a total of 40 muscles involved in driving the shoulder complex. The maximum strength of each muscle was estimated from the volume and length of the muscle. In this paper, the effect of the ligaments was verified by performing raising movement experiments with and without the ligaments, and the uniformity of the load on each muscle by distributing the maximum muscle force was verified by performing raising movement experiments when the maximum muscle force of each muscle was estimated and when it was averaged.

[1] The authors are with the Department of Mechano-Informatics, Graduate School of Information Science and Technology, The University of Tokyo, 7-3-1 Hongo, Bunkyo-ku, Tokyo, 113-8656, Japan. [sahara, miki, ribayashi, yoshimura, kawaharazuka, k-okada, inaba]@jsk.t.u-tokyo.ac.jp

II. Configuration of the Musculoskeletal Model of the Shoulder Complex

In this study, it was necessary to use a simulator capable of simulating a musculoskeletal model with ligaments. Since both muscles and ligaments are soft tissues, and muscles generate tension rather than torque like motors, a simulator that can accurately represent these characteristics was required. Additionally, the simulation speed was important when conducting robot simulations.

Based on these considerations, this study utilized MuJoCo as the simulator [6]. MuJoCo is a general-purpose physics engine intended to facilitate research and development in robotics, biomechanics, computer graphics and animation, machine learning, and other areas requiring fast and accurate simulation of articulated structures interacting with their environment. It can handle models containing tendons and muscles for simulations of tendon-driven robots such as musculoskeletal humanoids. Its simulation speed and accuracy are known to be superior to other mechanics simulators [7]. Based on the above reasons, MuJoCo was employed in this study.

The appearance of the musculoskeletal model of the shoulder complex created in this study is shown in Fig. 1. With the goal of creating a simulation model of the human shoulder complex with soft tissue ligaments and the same number of muscles as a human, this model was composed of three elements: skeleton, ligaments, and muscles. In this chapter, each of these elements is explained.

A. Linked structure of the skeleton

This model was constructed by the bones that make up the shoulder complex: thorax, spine, scapula, clavicle, and humerus. Of these, the thorax and spine, which are included in the torso, are fixed to the world coordinate system, while the scapula, clavicle, and humerus, which are involved in shoulder motion, are connected by using the structural joints, the sternoclavicular joint, acromioclavicular joint, and scapulohumeral joint, as spherical counterpart joints.

The links that compose this model were made using the skeletal mesh files provided by BodyParts3D [8]. BodyParts3D is a database developed by the Life Science Database Integration Project that describes the location and shape of human body parts (organs and organs) indicated by anatomical terms in a three-dimensional human body model. In addition to mesh files for the skeleton, it also provides mesh files for muscles and major organs, which were adopted because they could be used for judging skeletal hits and setting muscle attachment points.

We attempted to construct the degrees of freedom of each joint based on bone-to-bone contact, but because it was difficult for MuJoCo to determine the concave surface contact, we modeled the joints as spherical counterpart joints. Therefore, this model could not reproduce phenomena caused by translational movement such as shoulder dislocation.

TABLE I: List of ligaments in the musculoskeletal model. The "start" and "stop" are bones with end points of ligaments.

name	start	stop
Lig. interclaviculare	manubrium	clavicle
Lig. stemoclaviculare antarius	manubrium	clavicle
Lig. stemoclaviculare posterius	manubrium	clavicle
Lig. acromioclaviculare	clavicle	scapula
Lig. trapezoideum	clavicle	scapula
Lig. coracohumerale	clavicle	scapula
Ligamenta glenohumeralia	scapula	humerus

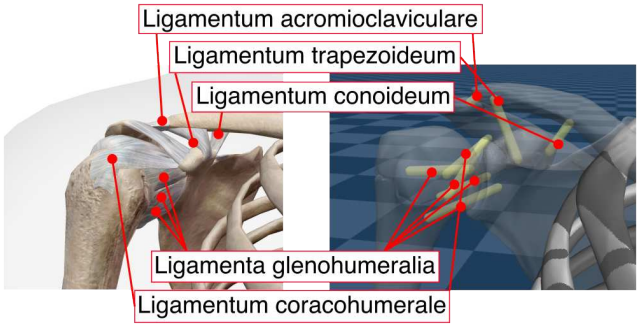

(a) Ligaments. The yellow wire on right figure is the ligament.

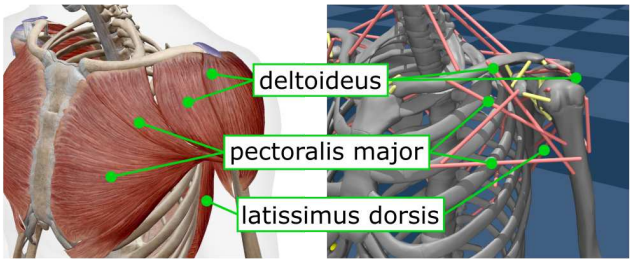

(b) Muscles. The red wire on right figure is the muscle.

Fig. 2: Overview of the comparison between human and musculoskeletal models. The left figure shows the human from Visible Body , and the right figure shows the musculoskeletal model developed in this study.

B. Representation and placement of ligaments

Human bones are connected to each other by ligaments. Ligaments are connective tissues that bind bone to bone and are elastic biological soft tissues. It is mainly composed of collagen and has the role of maintaining the relative positional relationship between bones and joint stability through its elasticity. In this study, ligaments were represented as elastic wires. The elastic wires were placed as shown in Fig. 2(a), based on the ligament and skeletal diagrams in Visible Body [9]. A list of the placed ligaments and the bones at both ends to which each ligament attaches is shown in Table I. MuJoCo's tendon element was used as the elastic wire. In Visible Body, the ligaments and skeleton are shown in 3D, but their coordinates, etc., are not specifically indicated, so the coordinates of the end points of each ligament were determined visually, referring to the diagram of the ligaments in Visible Body. Although some ligaments

TABLE II: List of muscles in the musculoskeletal model. The "origin" and "insertion" are bones with end points of muscles.

name	origin	insertion
pectoralis major	thorax	humerus
pectoralis minor	thorax	scapula
subscapularis	scapula	humerus
infraspinatus	scapula	humerus
teres major	scapula	humerus
teres minor	scapula	humerus
serratus anterior	thorax	scapula
pectoralis major pars clavicularis	clavicle	humerus
latissimus dorsi	thorax	humerus
deltoideus pars spinalis	scapula	humerus
deltoideus pars acriminalis	scapula	humerus
deltoideus pars clavicularis	clavicle	humerus
supraspinatus	scapula	humerus
platysma	thorax	clavicle
levator scaplulae	thorax	scapula
rhomboideus minor	thorax	scapula
rhomboideus major	thorax	scapula
descending part of trapezius	thorax	clavicle
transverse part of trapezius	thorax	scapula
ascending part of trapezius	thorax	scapula

do not constrain the positional relationship between bones, such as the transverse suprascapular ligament that forms the suprascapular foramen where the nerve passes, such ligaments were omitted in this model, and only ligaments that connect the different bones were placed. Since the glenohumeral ligament surrounds the humeral head of the scapulohumeral joint, it was represented by creating a sphere of the same shape as the humeral head and wrapping it around it. In this model, each joint was modeled as a spherical counterpart joint, so these ligaments were expected primarily to represent a range of motion equivalent to that of a human and to represent joint suppleness.

C. Representation and placement of muscles

Human skeletal muscles can be regarded as actuators between bones that generate tension. Bones and muscles are connected by tendons. Muscles are activated by electrical signals from nerves to generate tension, and mathematical models such as cross-bridge models [10] and Hill-type models [11] and other mathematical models exist to describe this behavior. The former model is based on the basic structure inside the muscle, but there are many parameters that must be identified, and many simulators use Hill-type models [12].

In this study, Hill-type models were used to represent muscles. The muscles involved in driving the shoulder complex were placed as shown in Fig. 2(b). A list of the placed muscles and the origin and stop of each muscle attachment is shown in Table II. The tendon and muscle elements of MuJoCo were used as muscles.

Humans have approximately 640 muscles. Since this study focuses only on the shoulder complex, 40 muscles that drive the scapula, humerus, and clavicle were selected. The way the muscles are classified varies somewhat in the literature, but in this study we followed the mesh file of the muscles contained in the BodyParts3D. Therefore, some muscles, such as the trapezius, were divided into multiple regions, and independent muscles were placed for each region in this model. The endpoints of each muscles were placed at the starting and stopping points of the muscles, respectively, referring to the mesh files of the muscles in BodyParts3D. Since both the starting and stopping points are not simple points but are in plane contact with the bone, in this model, they were placed at coordinates near the center of the plane by referring to the mesh file of the muscles. In addition, some muscles, such as the deltoid and pectoralis major, generate torque on the bone by wrapping around it. A cylinder was placed in the same position as the humerus, and muscles were wrapped around this cylinder to represent the wrapping of the muscles around the bone.

In the muscle element of MuJoCo, there exists a parameter that sets the maximum muscle force. It is known that there is a proportional relationship between the maximum muscle force and physiological cross-sectional area of human muscles such that Eq. 1 [13].

$$F = k_{stress} \cdot \mathrm{PCSA} \tag{1}$$

$$\mathrm{PCSA} = \frac{V}{l} \cdot \cos\alpha \tag{2}$$

$$V = \frac{m}{\rho} \tag{3}$$

F is the maximum muscle force, k_{stress} is the proportionality constant, and PCSA is the physiological cross-sectional area of the muscle. The physiological cross-sectional area is defined by Eq. 2, where V is muscle volume, l is muscle length, α is feather angle, m is muscle mass, and ρ is muscle density. This allows us to estimate the maximum muscle force if the muscle volume and length are known. In this model, the maximum muscle force was estimated by defining the muscle volume V by the volume of the mesh file provided by BodyParts3D and the muscle length l by the length of the tendon element on the model. The proportionality constant k_{stress} was set to the literature value $59\,\mathrm{Pa}$ [14].

III. Position control by model predictive control

The model developed had 40 muscles, making it a multi-input system. To see if this could be controlled, positional control of the elbow tip was performed. Because human muscles are arranged in an antagonistic manner, they can maintain their position even if extra muscular force is exerted between antagonistic muscles. However, exerting extra muscular force is thought to promote muscle fatigue, which is considered to be detached from actual human movement. Therefore, in this study, optimal control was employed to suppress unnecessary muscle fatigue. As a modeling method for muscle fatigue, there exists a model focusing on motor units proposed by Liu et al [15]. According to this model, muscle fatigue is calculated by the differential equation between muscle fatigue and the signal input to the muscle; the greater the signal to the muscle, the more muscle fatigue accumulates. Therefore, the objective of reducing muscle fatigue was substituted by simply decreasing the signal sent to the muscle.

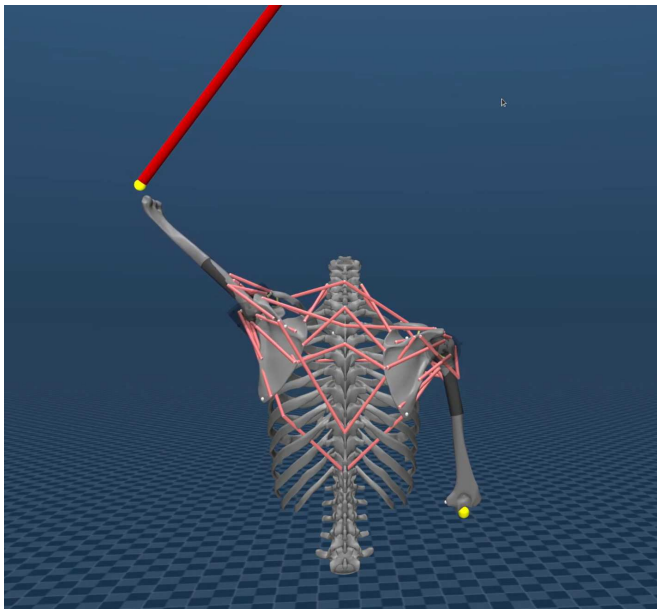

Fig. 3: Position control of the proposed musculoskeletal model with MPC. The two yellow balls are the target positions. The muscles are controlled to bring the tip of the humerus closer to the target position.

In this study, model predictive control was employed to achieve optimal control in a multi-input system. As an experimental environment, we used the software MuJoCo MPC, which is capable of model predictive control on the CPU [16]. MuJoCo MPC is software for online model predictive control on MuJoCo. By setting the model and cost function, control can be performed on MuJoCo through model predictive control. The target position was set by a yellow ball, and by moving this, it was checked whether the elbow tip would follow. In MuJoCo MPC, optimal control is performed such that the cost function is minimized. The cost function J is defined as the sum of the cost with respect to the position $\boldsymbol{p}$ and the cost with respect to the control input $\boldsymbol{u}$ with weights w_i as shown in Eq. 4.

$$J = \sum_i w_i \cdot r_i \tag{4}$$

$$r_1 = ||\boldsymbol{p}_{\text{target}} - \boldsymbol{p}_{\text{endeffector}}|| \tag{5}$$

$$r_2 = ||\boldsymbol{u}||^2 \tag{6}$$

Eq. 5 is a constraint on position, with the distance between the end-effector and the target position as the cost. $\boldsymbol{p}_{\text{target}}$ is the target position and $\boldsymbol{p}_{\text{endeffector}}$ is the end-effector position. In this study, the end-effector position was set at the tip of the humerus. Eq. 6 is a constraint on the control input, and the cost is the sum of squares of the vector $\boldsymbol{u} \in [0, 1]^{40}$ that lines up the signals to the 40 muscles in the model.

IV. Experiments with position control

A. Movement experiment by position control of elbow tip

We verified that the implemented elbow tip position control works correctly. It was confirmed that the elbow tip followed the yellow ball, which was set as the target position, by moving it manually. This is shown in Fig. 3. When the model's arm is moved by position control, its range of motion should be equivalent to that of a human. The human shoulder can be raised approximately 180 degrees forward, 180 degrees laterally, and 50 degrees backward [17]. Therefore, we checked to what extent the shoulder could be raised in this model anteriorly, laterally, and posteriorly, respectively. For each direction, the shoulder is shown in Fig. 4 when it is elevated. Here, the target position was set for each angle of elevation, and the state was observed after the shoulder was elevated and a short wait was made for the position to stabilize. Fig. 4(a) shows the state when the arm is raised laterally, Fig. 4(b) shows the state when the arm is raised forward, and Fig. 4(c) shows the state when the arm is raised backward. This confirms that the range of motion in both directions is comparable to that of a human.

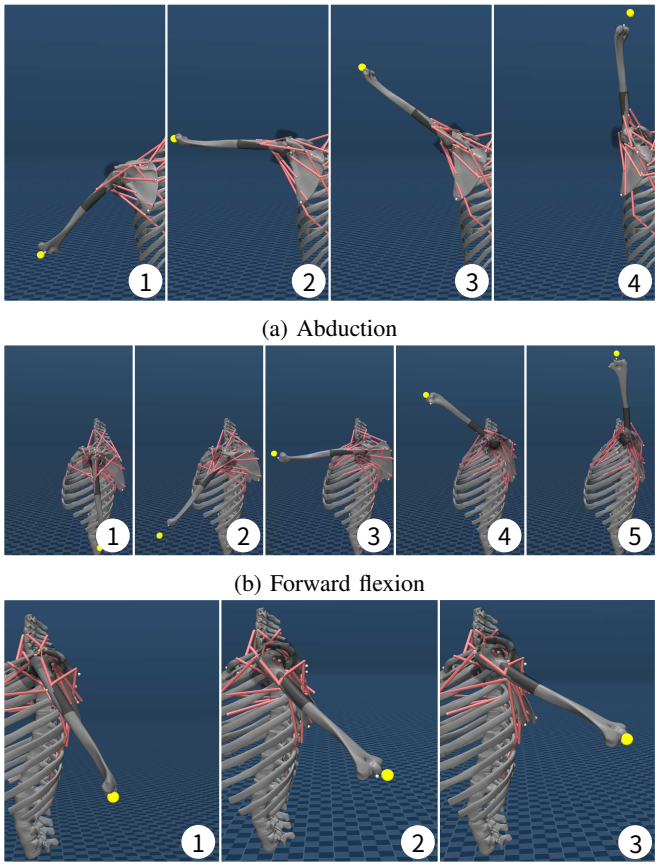

(a) Abduction

(b) Forward flexion

(c) Backward extension

Fig. 4: Elevation movements with MPC. As in humans, approximately 180 degrees of abduction, 180 degrees of anterior flexion, and 50 degrees of posterior flexion can be observed.

B. Raising movement experiment with and without ligaments

To see how the joint range of motion limitation of the ligament affects the raising of the upper arm, an experiment was conducted in which the elbow was raised with and

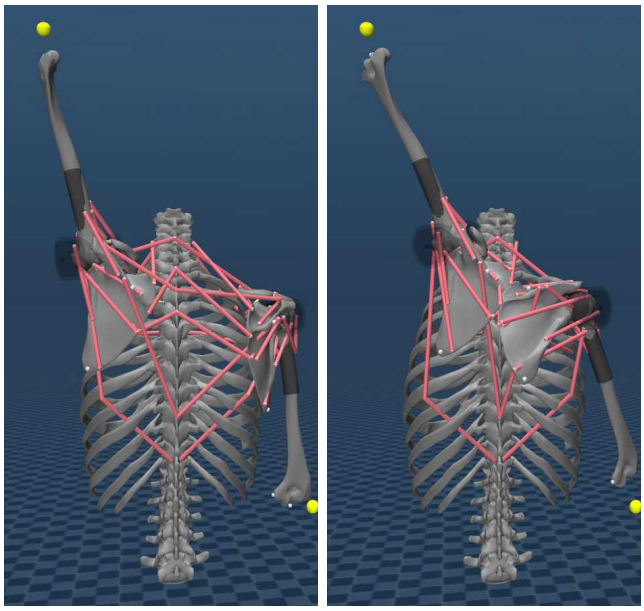

(a) With ligaments (b) Without ligaments

Fig. 5: Comparison of the elevation of the upper arm with and without ligaments. The position of the scapula is closer to the spine when the ligaments are absent.

without the ligament, respectively. By setting the target position above the left shoulder, the model was placed in an elevated posture. After the elbow was raised, the model waited until the posture became stable, and then was observed. The situation is shown in Fig. 5. Compared to when the ligaments were present, when the ligaments were absent, the position of the scapula was closer to the spine. The elimination of the ligaments has increased the range of motion of the sternoclavicular and acromioclavicular joints, allowing the shoulder to be positioned closer to the center of the body. This is thought to be due to the fact that the weight of the shoulder is now more easily deposited on the body.

The angles of the clavicle, scapula, and humerus during the raising motion are also shown in Fig. 6. This shows that the angular changes of the scapula and clavicle are more oscillatory when the ligaments are absent than when they are present, indicating that the lack of range-of-motion restriction by the ligaments makes that movement unstable.

C. Raising movement experiment with estimated and averaged maximum muscle force

In this model, the maximum muscle force of each muscle was estimated from muscle volume and length. In order to confirm how this maximum muscle force affects the upper arm raising motion, an experiment was conducted to raise the elbow when the maximum muscle force was estimated from the muscle volume and when it was averaged. Since maximal muscle force is proportional to muscle volume, averaging it corresponds to redistributing the muscle volumes of each muscle so that they are equal while maintaining the total

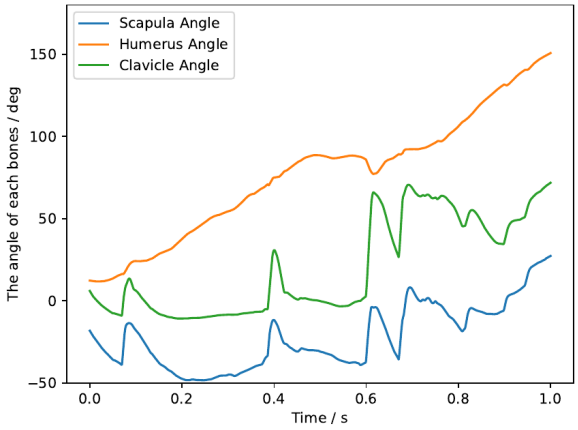

(a) Without ligaments

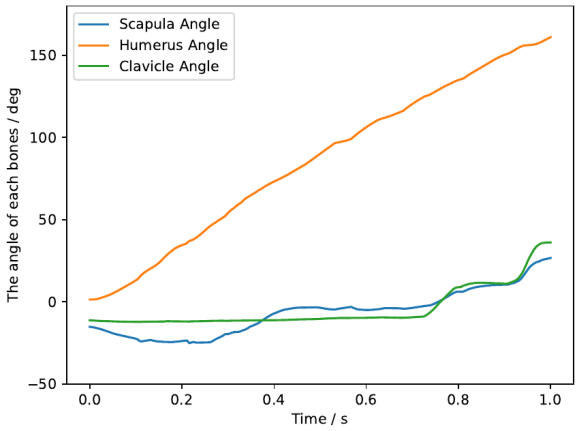

(b) With ligaments

Fig. 6: Angle of rotation of scapula, clavicle, and humerus during raising motion.

muscle volume of each muscle. The maximum muscle force estimated from the muscle volume and the maximum muscle force when averaged are shown in Table III.

An experiment was conducted in which the target position was moved in a semicircle around the shoulder to raise the upper arm over a period of one second. Eight trials were made for each of the times when the maximum muscle force was estimated from muscle volume, etc. and when it was averaged, and the tension force applied to the muscle at this time was recorded. The ratio of the recorded tension divided by the maximum muscle force was calculated, and the average μ is shown in Fig. 7. In addition, the standard deviation σ at each time is shown by coloring the area included in $[\mu - \sigma, \mu + \sigma]$. This shows that some muscles have a larger ratio of tension to maximum muscle force when averaged than when maximum muscle force is estimated from muscle volume and when averaged. In particular, the tension ratio is larger in muscles such as the serratus anterior, levator scapulae, and descending trapezius. For the serratus

TABLE III: Maximum muscle forces in the musculoskeletal model. EMF is estimated muscle force, and AMF is average muscle force. The underlined values are higher than the average muscle force.

muscle	EMF / N	AMF / N
pectoralis major	445.0	276.9
pectoralis minor	23.0	276.9
subscapularis	417.0	276.9
infraspinatus	140.0	276.9
teres major	98.5	276.9
teres minor	79.6	276.9
serratus anterior	40.0	276.9
pectoralis major pars clavicularis	176.0	276.9
latissimus dorsi	197.0	276.9
deltoideus pars spinalis	32.6	276.9
deltoideus pars acriminalis	32.4	276.9
deltoideus pars clavicularis	118.0	276.9
supraspinatus	146.0	276.9
platysma	799.0	276.9
levator scaplulae	22.2	276.9
rhomboideus minor	35.2	276.9
rhomboideus major	30.0	276.9
descending part of trapezius	2626.0	276.9
transverse part of trapezius	32.1	276.9
ascending part of trapezius	48.2	276.9
total	5537.8	5537.8

anterior and levator scapulae muscles, the tension ratio is greater than 1, indicating that the muscles are being pulled and stretched fully.

The volume of human muscles differs from region to region, and this in turn causes the maximum muscle strength to differ. Larger muscles, i.e., those with greater maximal muscle strength, are considered to be those that require greater force in actual movement. By averaging the maximum muscle strength, the muscles that originally demanded greater strength would not be able to exert sufficient muscle strength, and in order to raise the arm in this state, a greater load would have been placed on other muscles.

In addition, the image after the model's upper arm is raised and stabilized is shown in Fig. 8. This shows that the position of the scapula is different when maximum muscle force is estimated from muscle volume and when it is averaged. When the maximum muscle force is averaged, the stable position of the scapula is shifted away from the spine. At Table III, the muscles with greater than average maximum muscle strength included the latissimus dorsi, pectoralis major, vastus lateralis, and subscapularis muscles. Among these muscles, the latissimus dorsi, pectoralis major, and subscapularis muscles all work to move the shoulder closer to the spinal column, so the smaller strength of these muscles is thought to have shifted the stable position of the shoulder blade away from the spine.

From these results, it was found that while the load on each muscle can be appropriately distributed by properly estimating the maximum muscle strength, conversely, if the maximum muscle strength is averaged, the muscles that are supposed to produce large force cannot exert sufficient force, and in order to raise the arm in that state, a large load is placed on other muscles, which also affects the posture in which the arm is raised.

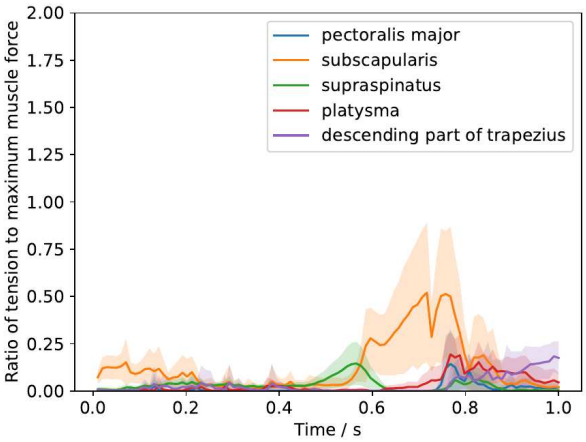

(a) Estimated

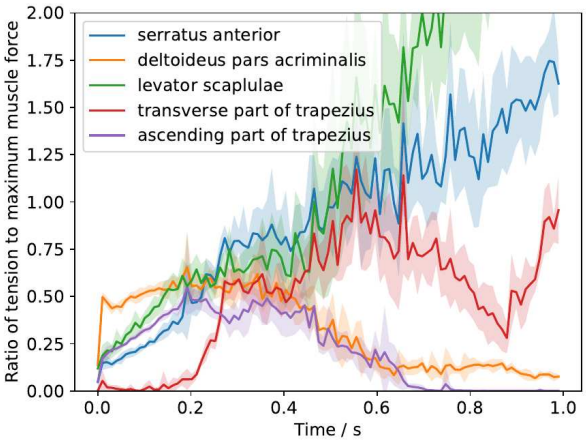

(b) Averaged

Fig. 7: Comparison of the transitions and distribution of muscle tension during the arm raising movement in the case of estimated and averaged muscle tension. For the mean μ and standard deviation σ of the muscle tension at each time during the 8 trials, the change in μ is represented by a line, and the distribution is shown by filling in the $[\mu - \sigma, \mu + \sigma]$ area.

V. Conclusion

In this study, ligaments were integrated into a musculoskeletal model of the human shoulder. The skeleton was treated as links, which were represented by mesh files scanned from a human skeleton, and structural joints were represented by spherical counterparts. Ligaments were implemented in spherical-dual joints primarily to limit the range of motion of the joints. The position of the ligaments was determined with reference to the arrangement of human ligaments, and these were represented by elastic wires. Muscles were placed based on human muscle mesh files, and their maximum muscle strength was estimated from muscle volume and length.

Although the model created was a multi-input system

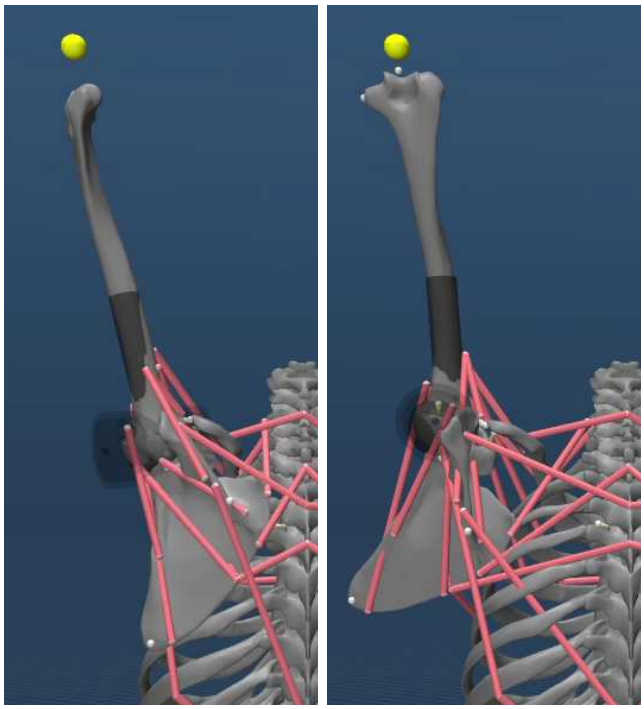

(a) Estimated (b) Average

Fig. 8: Comparison of maximum muscle strength estimated from muscle volume and length and averaged. The scapula is further away from the spine in the averaged case than in the estimated case.

with 40 muscles in both shoulders, position control of the elbow tip was achieved by model predictive control that added signal input to the muscles to the evaluation function. Using positional control, we investigated the changes in posture by changing the presence or absence of ligaments and the distribution of muscle force in the upper arm raising movement. When the ligaments were removed, the joint range of motion was no longer restricted, the position of the scapula during raising was closer to the spine, and the angles of each bone during the raising motion showed unstable changes. In addition, when maximum muscle force was estimated from muscle volume and averaged, the load on each muscle was more distributed in the former case, and in the latter case, muscles with a larger ratio of muscle tension to maximum muscle force occurred. This may suggest that muscles that are thicker and have greater maximal muscle force are those that require greater force in human exercise.

In the future, the developed simulation model could be used to examine how muscles should be used in more practical tasks in sports and martial arts by optimizing their movement. Also, in the design and control of musculoskeletal humanoids, it would be possible to reduce unnecessary output and price by using ligaments for joint configuration and by making its muscles high-power actuators for the larger muscles in the human body and low-power actuators for those that are not.

REFERENCES

[1] K. R. Holzbaur, W. M. Murray, and S. L. Delp, "A model of the upper extremity for simulating musculoskeletal surgery and analyzing neuromuscular control," *Annals of biomedical engineering*, vol. 33, pp. 829–840, 2005.

[2] J. De Groot and R. Brand, "A three-dimensional regression model of the shoulder rhythm," *Clinical biomechanics*, vol. 16, no. 9, pp. 735–743, 2001.

[3] C. Vittorio, W. Huawei, D. Guillaume, S. Massimo, and K. Vikash, "Myosuite – a contact-rich simulation suite for musculoskeletal motor control," https://github.com/facebookresearch/myosuite, 2022. [Online]. Available: https://arxiv.org/abs/2205.13600

[4] Y. Asano, T. Kozuki, S. Ookubo, M. Kawamura, S. Nakashima, T. Katayama, Y. Iori, H. Toshinori, K. Kawaharazuka, S. Makino, Y. Kakiuchi, K. Okada, and M. Inaba, "Human Mimetic Musculoskeletal Humanoid Kengoro toward Real World Physically Interactive Actions," in *Proceedings of the 2016 IEEE-RAS International Conference on Humanoid Robots*, 2016, pp. 876–883.

[5] K. Kawaharazuka, S. Makino, K. Tsuzuki, M. Onitsuka, Y. Nagamatsu, K. Shinjo, T. Makabe, Y. Asano, K. Okada, K. Kawasaki, and M. Inaba, "Component Modularized Design of Musculoskeletal Humanoid Platform Musashi to Investigate Learning Control Systems," in *Proceedings of the 2019 IEEE/RSJ International Conference on Intelligent Robots and Systems*, 2019, pp. 7294–7301.

[6] E. Todorov, T. Erez, and Y. Tassa, "Mujoco: A physics engine for model-based control," in *Proceedings of the 2012 IEEE/RSJ International Conference on Intelligent Robots and Systems*, 2012, pp. 5026–5033.

[7] T. Erez, Y. Tassa, and E. Todorov, "Simulation tools for model-based robotics: Comparison of bullet, havok, mujoco, ode and physx," in *Proceedings of the 2015 IEEE International Conference on Robotics and Automation*. IEEE, 2015, pp. 4397–4404.

[8] N. Mitsuhashi, K. Fujieda, T. Tamura, S. Kawamoto, T. Takagi, and K. Okubo, "Bodyparts3d: 3d structure database for anatomical concepts," *Nucleic acids research*, vol. 37, no. suppl_1, pp. D782–D785, 2009.

[9] A. Publishing, "Visible body," 2018.

[10] E. Eisenberg, T. L. Hill, and Y.-d. Chen, "Cross-bridge model of muscle contraction. quantitative analysis," *Biophysical Journal*, vol. 29, no. 2, pp. 195–227, 1980.

[11] T. L. Hill, "Theoretical formalism for the sliding filament model of contraction of striated muscle part i," *Progress in biophysics and molecular biology*, vol. 28, pp. 267–340, 1974.

[12] M. Millard, T. Uchida, A. Seth, and S. L. Delp, "Flexing Computational Muscle: Modeling and Simulation of Musculotendon Dynamics," *Journal of Biomechanical Engineering*, vol. 135, no. 2, p. 021005, 02 2013. [Online]. Available: https://doi.org/10.1115/1.4023390

[13] R. S. Sopher, A. A. Amis, D. C. Davies, and J. R. Jeffers, "The influence of muscle pennation angle and cross-sectional area on contact forces in the ankle joint," *The Journal of Strain Analysis for Engineering Design*, vol. 52, no. 1, pp. 12–23, 2017, pMID: 29805194. [Online]. Available: https://doi.org/10.1177/0309324716669250

[14] R. Hale, D. Dorman, and R. V. Gonzalez, "Individual muscle force parameters and fiber operating ranges for elbow flexion – extension and forearm pronation – supination," *Journal of Biomechanics*, vol. 44, no. 4, pp. 650–656, 2011. [Online]. Available: https://www.sciencedirect.com/science/article/pii/S0021929010006330

[15] J. Z. Liu, R. W. Brown, and G. H. Yue, "A dynamical model of muscle activation, fatigue, and recovery," *Biophysical journal*, vol. 82, no. 5, pp. 2344–2359, 2002.

[16] T. Howell, N. Gileadi, S. Tunyasuvunakool, K. Zakka, T. Erez, and Y. Tassa, "Predictive Sampling: Real-time Behaviour Synthesis with MuJoCo," dec 2022. [Online]. Available: https://arxiv.org/abs/2212.00541

[17] I. Kapandji, *The Physiology of the Joints: The upper limb*, ser. The Physiology of the Joints. Churchill Livingstone, 2007.